International Journal of Pharmaceutics 416 (2011) 110–119

Contents lists available at ScienceDirect

International Journal of Pharmaceutics

journal homepage: www.elsevier.com/locate/ijpharm

Combining experimental design and orthogonal projections to latent structures to study the influence of microcrystalline cellulose properties on roll compaction

Melanie Dumarey[a], Håkan Wikström[b], Magnus Fransson[b], Anders Sparén[b], Pirjo Tajarobi[b], Mats Josefson[b,*], Johan Trygg[a]

[a] Computational Life Science Cluster (CLiC), Department of Chemistry, Umeå University, Sweden
[b] Pharmaceutical Development, AstraZeneca R&D Mölndal, Sweden

ARTICLE INFO

Article history:
Received 5 April 2011
Received in revised form 9 June 2011
Accepted 11 June 2011
Available online 17 June 2011

Keywords:
Experimental design
Microcrystalline cellulose
Orthogonal projections to latent structures
Principal component analysis
Roll compaction
Tablet manufacturing

ABSTRACT

Roll compaction is gaining importance in pharmaceutical industry for the dry granulation of heat or moisture sensitive powder blends with poor flowing properties prior to tabletting. We studied the influence of microcrystalline cellulose (MCC) properties on the roll compaction process and the consecutive steps in tablet manufacturing. Four dissimilar MCC grades, selected by subjecting their physical characteristics to principal components analysis, and three speed ratios, i.e. the ratio of the feed screw speed and the roll speed of the roll compactor, were included in a full factorial design. Orthogonal projection to latent structures was then used to model the properties of the resulting roll compacted products (ribbons, granules and tablets) as a function of the physical MCC properties and the speed ratio. This modified version of partial least squares regression separates variation in the design correlated to the considered response from the variation orthogonal to that response. The contributions of the MCC properties and the speed ratio to the predictive and orthogonal components of the models were used to evaluate the effect of the design variation. The models indicated that several MCC properties, e.g. bulk density and compressibility, affected all granule and tablet properties, but only one studied ribbon property: porosity. After roll compaction, Ceolus KG 1000 resulted in tablets with obvious higher tensile strength and lower disintegration time compared to the other MCC grades. This study confirmed that the particle size increase caused by roll compaction is highly responsible for the tensile strength decrease of the tablets.

1. Introduction

Roll compaction is a well established technique involved in many industrial processes (Johanson, 1965; Dec et al., 2003) as for instance the rolling of metal strips. Recently, it is gaining importance in the dry granulation of pharmaceutical powder blends with poor flowing properties not suited for wet granulation (Bindhumadhavan et al., 2005; Kleinebudde, 2004; Jeon et al., 2009). In this type of applications the feeding screw of the roll compactor directs the powder towards the gap between two counter rotating rolls, where the powder is compacted with a continuous, very high pressure into flakes or ribbons. These products are then milled to obtain granules with improved flow properties (Johanson, 1965; Kleinebudde, 2004). Since a liquid binder is not required in this process and as a consequence also a drying step is superfluous, this type of granulation is extremely valuable for heat or moisture sensitive components (Bindhumadhavan et al., 2005; Kleinebudde, 2004). A slight drawback is the loss in compactibility after roll compaction (Malkowska and Khan, 1983).

Most studies on roll compaction in the pharmaceutical field are focusing on understanding and optimizing the process parameters. Johanson (1965) started this work by developing the rolling theory for granular solid, which enabled the prediction of the exerted press in the roll compactor from the flow properties of the solid, roll size, roll gap, roll surface condition and feed pressure. This model was later compared with newer slab method based and final element models by Dec et al. (2003). A more practical application of Johanson's model was studied by Reynolds et al. (2010), who modeled the ribbon density as a function of the process parameters. Falzone et al. (1992) built quadratic regression models for different powders to describe both the particle size distribution and the recompressibility of the granules as a function of the applied roll speed, horizontal feed speed and vertical feed speed. These models helped to select compactor parameters levels resulting in successful tablet production. However, no general model for all considered powders could be established. Farber et al. (2008) described the relation between the applied roll compaction conditions and the tensile strength of the resulting tablets. Their model assumes that compaction is cumulative during

* Corresponding author. Tel.: +46 31 7761658.
E-mail address: mats.josefson@astrazeneca.com (M. Josefson).

0378-5173/$ – see front matter © 2011 Elsevier B.V. All rights reserved.
doi:10.1016/j.ijpharm.2011.06.018

roller compaction and subsequent granule compaction, and consequently tablets compressed from the resulting granulation are weaker than those compressed by direct compression at the same compression force. Am Ende et al. (2008) improved the content uniformity of a low dose tablet formulation by optimizing the roll force and the gap width of the roll compactor using experimental design.

However, only a few papers have been published describing the relation between raw material properties and roll compacted products. In a study of Bacher et al. (2007), it was revealed that the calcium carbonate morphology and sorbitol particle size were more influential on the compaction properties than the settings of the roll compactor. When Herting and Kleinebudde (2007) studied the effect of binder (microcrystalline cellulose, MCC) and active compound (theophylline) particle size on roll compaction, they observed that MCC with smaller particle size resulted in larger granules with better flowability and tablets with higher tensile strength. The same authors also studied the tensile strength of MCC containing tablets after roll compaction and concluded that both particle size enlargement and hardening of the material are responsible for the reduction of the tensile strength after roll compaction (Herting and Kleinebudde, 2008). However, Sun and Himmelspach (2006) claimed that this phenomenon could be explained by granule size enlargement alone. Bultmann (2002) observed that the multiple compaction of MCC in a roller compactor reduced the amount of fines produced during compaction. The mean particle size, flow properties and bulk density of the granules increased, while their size distribution improved. This study also confirmed the decreased tensile strength of tablets after roll compaction.

The objective of this study is to evaluate the influence of a broad range of raw material properties from powder rheometry as well as density and particle size distribution on the different products (ribbons, granules and tablets) obtained after roll compaction, milling and tabletting, using innovative multivariate approaches (Fig. 1). Fillers, i.e. inert powders added to the active compound to increase bulk volume and drug availability, mostly constitute the largest fraction of a tablet and can exhibit considerate differences in physical properties. Therefore, in this study the grade of MCC, a common pharmaceutical filler, was varied in a full factorial design (FFD) as well as the ratio roll speed/feed screw speed of the roll compactor (ratio). The qualitative factor MCC grade was then expressed as several quantitative powder properties for the development of orthogonal projections to latent structures (OPLS) (Trygg and Wold, 2002) models describing the individual properties of the different roll compacted products. OPLS, a modified version of partial least squares (PLS), can separate the design variation related to the product property from the unrelated variation, which results in less complex models with improved interpretability, e.g. the powder properties not affecting the roll compaction, can be indicated. Finally, also the differences between roll compacted and direct compressed tablets were studied.

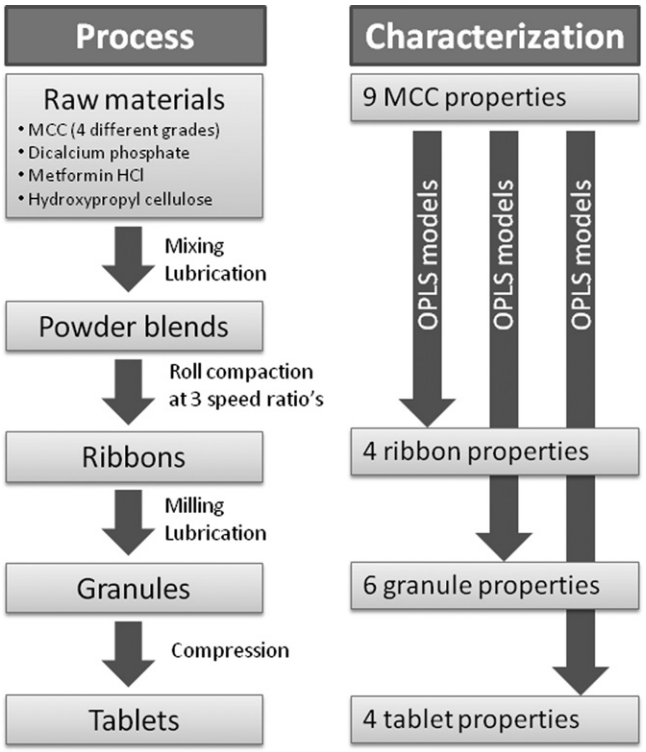

Fig. 1. The studied tablet manufacturing process with the applied design variation visualized in the left part of the figure, while the corresponding characterization and modeling strategy are shown in the right part.

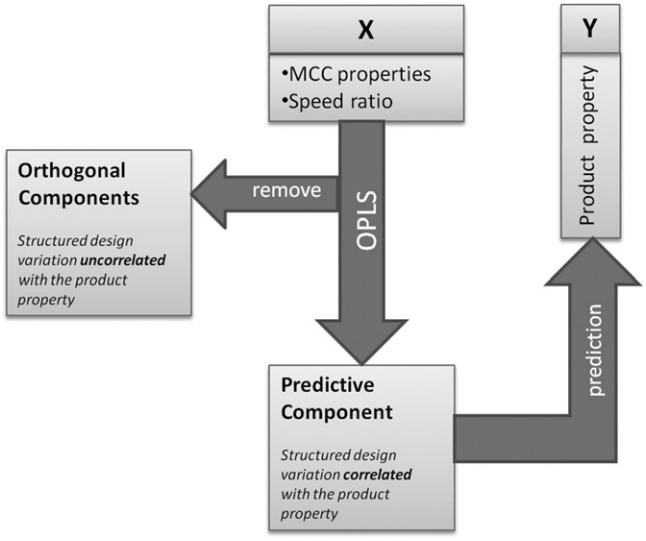

Fig. 2. Overview of the OPLS method, which separates the predictive and orthogonal variation in the descriptive data (X) for the modeling of a response (Y).

2. Theory

2.1. Orthogonal projections to latent structures

In partial least squares (PLS) the NIPALS algorithm can be used to model a property (**y**) as a function of many descriptor variables, organized in a matrix (**X**), maximizing the covariance between **X** and **y** (Massart et al., 1998). In OPLS (Trygg and Wold, 2002), however, this NIPALS algorithm is slightly modified in order to calculate orthogonal components, which contain the structured variation in **X** not related with **y** (Fig. 2). This produces score and loading plots, which are easier to interpret and offers the advantage that the orthogonal variation in **X** can be analyzed separately. Practically, the variables with high, significant loadings on the predictive component are strongly related with **y**, while the variables with high loadings on the orthogonal components exhibit a large amount of structured variation unrelated to **y**. The R^2X value for the predictive component represents the fraction of variation in **X** related to **y**, while for the orthogonal component it represents the structured variation not related to **y**. A low R^2X value for the predictive component indicates thus that **X** contains much variation not related to **y**. The R^2Y value is the correlation between the measured and predicted **y** values and gives an indication how well the model describes the response. The predictive ability of the model can be

Table 1
Full factorial design to study the influence of MCC grade and ratio of roll speed and feed screw speed (ratio) on roll compaction (RC). The roll speed of the roll compactor was set to 3 rpm and the feed screw speed to 18, 24 or 30 rpm (based on the ratio in the design). A pressure of 5 MPa was applied on the rolls.

RC formulation	MCC grade	Ratio
1	Avicel PH101	6
2	Avicel PH101	10
3	Avicel PH105	6
4	Avicel PH105	10
5	Avicel PH200	6
6	Avicel PH200	10
7	Ceolus KG 1000	6
8	Ceolus KG 1000	10
9	Avicel PH101	8
10	Avicel PH101	8
11	Avicel PH101	8

estimated by Q^2, i.e. the correlation between the measured **y** values and those predicted with cross validation models.

Despite the separation of predictive and orthogonal variation by OPLS, PLS and OPLS models cover identical model space for a single response, given that they contain the same number of components. Practically, this implies that the describing and predictive capacities of both model types are identical (similar R^2Y and Q^2 values) for a single response and they only differ in interpretational abilities.

In experimental design, the use of OPLS is more advantageous if the design factors exhibit a high degree of correlation and/or if the causality between the factors and the response is not clear. However, OPLS is not beneficial for full factorial designs in which the factors are by definition orthonormal, because the models will contain one predictive component identical to the corresponding multiple linear regression model.

When multiple responses are included in an OPLS model, the model space available for orthogonal variation will be reduced and the interpretability of the predictive variation complicated. Therefore it is recommended to construct separate OPLS models for each single response.

3. Experimental

3.1. Formulation

Fifteen tablet batches were produced: 11 roll compacted batches within the full factorial experimental design (shown in Table 1) directly compressed batches. Apart from the MCC grade, all batches had exactly the same composition: 15% metformin HCl BP/EP (Sohan Healthcare Pvt. Ltd., Wanowarie, India), 4% low-substituted hydroxypropyl cellulose LH 21 (L-HPC, Shin Etsu Chemical, Tokyo, Japan), 1% sodium stearyl fumarate (NaSF, Pruv, JRS Pharma GmbH & Co. KG, Rosenberg, Germany) and 80% of an MCC/dicalciumphosphate dihydrate (DCPD, Emcompress, JRS Pharma) mixture in a 70/30 ratio. The four MCC grades chosen for this study were Avicel PH101 (FMC BioPolymer, Philadelphia, PA, USA), Avicel PH105 (FMC Corporation, Newark, USA), Avicel PH 200 (FMC BioPolymer) and Ceolus KG 1000 (Asahi Kasei Chemicals Corporation, Tokyo, Japan). All weighed components, except NaSF, were mixed for five minutes with the Turbula mixer, type T2C (Willi A. Bachofen AG mashinen fabrik, Basel, Switzerland). Then 1% lubricant, NaSF, was added and the blend was mixed again with the Turbula mixer for 2 min.

3.2. Roll compaction

All batches produced within the design (Table 1) were roll compacted with the Vector TFC-Labo (Vector, Marion, IA, USA) using 24 mm wide die punch serrated rolls with a diameter of 50 mm. A pressure of 5 MPa was applied to the rolls, while the gap width was uncontrolled. The roll speed was set to 3 rpm and the feed screw speed was varied between 12, 24 and 30 rpm as described in Table 1. By applying different screw speeds in the design, it was possible to understand how the material was affected by different compaction forces. The roll speed is kept constant, because in literature (Hervieu et al., 1994; Teng et al., 2009) it was demonstrated that mainly the ratio of the roll speed and the feed screw speed influences the roll compacted products. Consecutively, the resulting ribbons were milled with a Vector TFC-Labo mill (Vector) using a 965 μm mill screen at a mill speed of 143 rpm.

3.3. Tabletting

Both the granules obtained from the roll compacted batches and the powder blends for direct compression were lubricated again with 1% NaSF for 2 min. The lubricated products were then compressed with the Korsch EK0 (Korsch GmbH, Berlin, Germany) at 5 different press forces (4, 8, 12, 16 and 20 kN) using a 8 mm flat, round punch aiming for 200 mg tablets. Eventually for each batch also 50 tablets were compressed at a press force resulting in tablets with a crushing strength approximating 80 N.

3.4. Powder and granule characterization

Thirteen MCC grades were characterized: Avicel PH 101, Avicel PH 102, Avicel PH 102 special coarse grade, Avicel HFE 102, Avicel PH105, Avicel PH 200, Emcocel 50, Prosolv 50, Prosolv 90, Prosolv 90 HD, Ceolus UF-711, Ceolus KG-802 and Ceolus KG-1000. The bulk density (BD), compressibility (Comp) and permeability (Perm) of the MCC grades, powder blends and granules were evaluated with a FT4 Powder rheometer (Freeman Technology, Welland, United Kingdom). The compressibility (%) and permeability (mbar) were recorded at an end stress of 15 kPa. The rheometer was also used to determine basic flowability energy (BFE), stability index (SI), specific energy (SE) and flow rate index (FRI) of the MCC. More information about the applied rheology methods can be found in Freeman (2007). The mass flow (F) of the granules and powder blends was measured with a flow meter (Erweka GmbH, Heusenstamm, Germany) using an orifice with 15 mm diameter and a stirrer speed of 2. The particle size diameter at the 10th and 50th percentile (psd1 and psd2) of the particle size distribution curve was measured with laser diffraction (Mastersizer 2000, Malvern Instruments Ltd., Malvern, United Kingdom) for the pure MCC grades, powder blends and granules. Practically, this measure means that 10% (or 50%) of the particles have a diameter psd1 (or psd2) or smaller. All the characterized properties and their abbreviations are listed in Table 2, while the actual characterization results and the MCC grade abbreviations are shown in Table 3. We acknowledge that the MCC characterization is limited and would be more complete including compactability and yield pressure. Including these measures could result in a different selection of MCC grades. However, the results of our study indicate an appropriate selection, since the design variation resulted in product variation.

3.5. Ribbon characterization

After roll compaction three properties were measured: the thickness of the ribbon (Th) with the caliper Absolute IP67 (Mitutoyo Corporation, Kawasaki, Japan), the envelope density of the ribbon (RD) with the Geopyc1360 (Micromeritics, Norcross, GA, USA) and the percentage of fines (Fin) produced during roll compaction (Table 2). The latter was measured by sieving (1.600 mm DIN4188 sieve, Retsch, Haan, Germany) the ribbons from the fines

Table 2
Abbreviations and units for properties measured of MCC, powder blends, ribbons, granules and tablets.

MCC	
BD	Bulk density (g/ml)
SE	Specific energy (mJ/g)
BFE	Basic flowability energy (mJ)
SI	Stability index
FRI	Flow rate index
Comp	End press compressibility (%)
Perm	Permeability (mbar)
psd1	Particle size distribution $d(0.1\,\mu m)$
psd2	Particle size distribution $d(0.5\,\mu m)$
Powder blend	
BDp	Bulk density (g/ml)
Fp	Mass flow (g/s)
Compp	End press compressibility (%)
Permp	Permeability (mbar)
psd1p	Particle size distribution $d(0.1\,\mu m)$
psd2p	Particle size distribution $d(0.5\,\mu m)$
Ribbon	
Th	Thickness (mm)
RD	Envelope density (g/ml)
Fin	Fines (%)
P	Porosity (%)
Granules	
BDg	Bulk density (g/ml)
Fg	Mass flow (g/s)
Compg	End press compressibility (%)
Permg	Permeability (mbar)
psd1g	Particle size distribution $d(0.1\,\mu m)$
psd2g	Particle size distribution $d(0.5\,\mu m)$
Tablets	
t_{dis}	Disintegration time (min)
RSDm	Relative standard deviation mass (%)
TS	Tensile strength (MPa) at 20 kN
TSn	Tensile strength of 80 N tablets normalized with compaction pressure multiplied by 1000
CU	Content uniformity (% RSD)

and weighing both separately. The porosity of the ribbons (P) was calculated according to

$$P = \left(1 - \left(\rho_e/\rho_t\right)\right) \times 100\% \quad (1)$$

where ρ_e is the envelope density of the ribbon and ρ_t the true density of the powder blend measured with the Accupyc 1330 (Micromeritics).

3.6. Tablet characterization

The tablet mass variation (RSDm) in each batch was expressed as the relative standard deviation percentage of the weight of ten of the tablets with a crushing strength of approximately 80 N. The same tablets were used for the evaluation of content uniformity (CU) with an isocratic HPLC method. The HPLC system (Alliance 2695, Waters Corporation, Milford, MA, USA) was operated with Empower 2 software (Waters Corporation) and contained a Dual λ Absorbance Detector 2487 (Waters Corporation) and a μBondapak C18 column (Waters Corporation) with dimensions 3.9 mm × 300 mm and particle size of 10 μm. The injection volume was set to 10 μl, the flow rate to 1 ml/min and the detection wavelength to 218 nm. The mobile phase, containing LiChrosolv acetonitrile (Merck KGaA, Darmstadt, Germany) and a buffer (10:90), was mixed online. The buffer contained 0.05% of each sodium 1-heptanesulfonate (Sigma Aldrich, Saint Louis, MO, USA) and sodium chloride (Scharlau, Sentmenat, Spain). 13.75 ml of a 1 M ortho-phosphoric acid (prepared from 85% ortho-phosphoric acid, Scharlau Chemie SA, Barcelona, Spain) solution was added before dilution with purified water (Milli-Q Gradient A10, Millipore Corporate, Billerica, MA, USA) to 5 l in order to obtain a pH between 3.8 and 3.9. Two metformin standards were prepared by dissolving 30 mg of metformin HCl in purified water and diluting to 100 ml. For the sample preparation 40 ml purified water was added to the tablet in a 100 ml volumetric flask, which was then shaken for 10 min. Consecutively, the volume was adjusted to 100.0 ml and the solution filtered through a PTFE membrane filter with diameter 25 mm and pore size 0.45 μm (Advantec MFS, Dublin, CA, USA). The chromatographic analysis took 12 min per sample and was performed at room temperature. Each analysis series started with the analyses of the two standards, followed by the injections of 10 samples. One standard was injected before the next series of 10 samples was started. A series was always ended with the injection of a standard. Eventually the content uniformity of each batch was calculated as the relative standard deviation (RSD) of the metformin concentration of the analyzed tablets. The tensile strengths (TS) of the tablets compressed at 5 different press forces and the tablets with an aimed crushing strength of 80 N were determined with the Multicheck Turbo III (Erweka GmbH). For each different press force ten tablets were measured and the average tensile strength was calculated. The maximum average tensile strength, which was obtained at 20 kN for each batch, was retained for modeling purposes, because we consider the pressure-strength relationships as rise-to-maximum exponential relationships. Six of the tablets with an aimed crushing strength of 80 N were used to measure the disintegration time (Erweka) of the different batches.

Table 3
Characteristics of the studied MCC grades ranked according to particle size. The abbreviations used for the MCC characteristics are listed in Table 2.

Trade name	Abbreviation	Vendor	BD (g/ml)	SE (mJ/g)	BFE (mJ)	SI	FRI	Comp (%)	Perm (mbar)	psd1 (μm)	psd2 (μm)
Avicel PH105	Av 105	FMC Biopolymer	0.36	11.8	104	0.96	2.69	24.4	5.2	7.2	22.2
Ceolus KG-1000	Ceo 1000	Asahi Kasei Chemicals Corp.	0.15	4.7	152	1.06	2.18	32.2	0.7	13.0	39.5
Ceolus UF-711	Ceo 711	Asahi Kasei Chemicals Corp.	0.27	8.1	220	0.99	1.66	19.7	0.7	16.4	45.6
Ceolus KG-802	Ceo 802	Asahi Kasei Chemicals Corp.	0.26	7.7	154	1.11	1.66	21.6	1.0	16.9	46.0
Prosolv 50	Pro 50	JRS Pharma	0.34	6.3	277	1.02	1.64	12.8	1.1	19.1	50.5
Avicel PH 101	Av 101	FMC Biopolymer	0.32	5.4	284	1.00	1.63	17.5	0.9	21.8	57.3
Emcocel 50	Em 50	JRS Pharma	0.30	6.8	243	1.02	1.58	16.9	0.8	22.5	59.9
Prosolv 90	Pro 90	JRS Pharma	0.36	4.4	184	1.06	1.32	10.2	0.7	27.7	98.3
Avicel PH 102	Av 102	FMC Biopolymer	0.34	5.5	268	0.95	1.46	13.3	0.6	35.7	115.1
Avicel HFE 102	Av hfe 102	FMC Biopolymer	0.42	4.8	256	1.04	1.37	9.2	0.7	33.7	117.9
Prosolv 90 HD	Pro 90 hd	JRS Pharma	0.42	5.7	256	1.01	1.52	7.1	0.7	56.2	143.4
Avicel PH 102 scg	Av 102 sg	FMC Biopolymer	0.38	5.1	220	1.00	1.46	10.2	0.7	38.7	143.9
Avicel PH 200	Av200	FMC Biopolymer	0.39	4.7	269	0.95	1.41	7.9	0.4	109.5	228.1

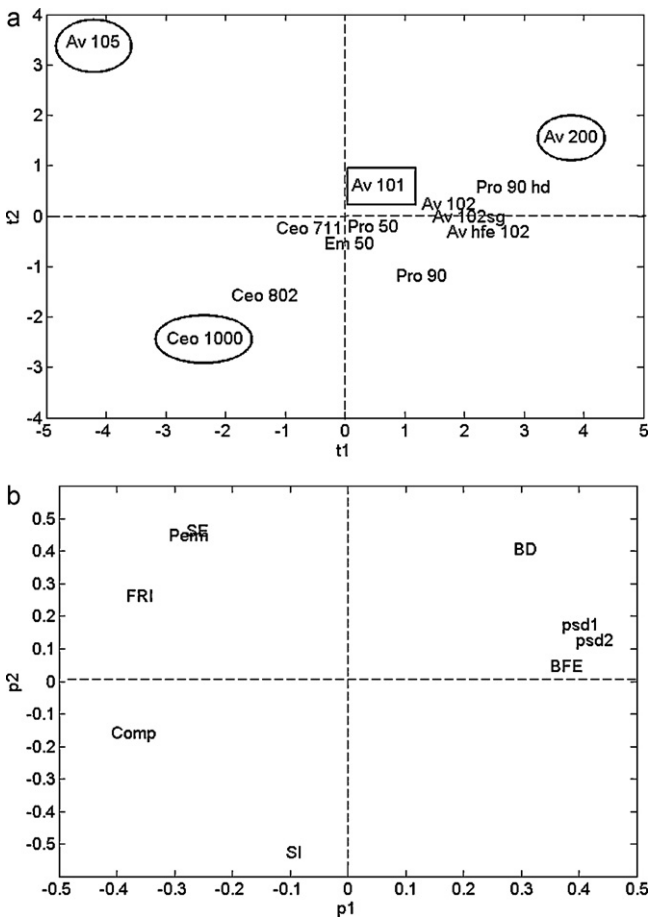

Fig. 3. (a) PC1–PC2 score plot of 13 MCC grades based on nine properties with the center point indicated by a rectangle and the three extreme grades by ellipses. The MCC grade abbreviations are listed in Table 3. (b) PC1–PC2 loading plot of the nine measured properties used to characterize 13 MCC grades. This plot indicates which properties are responsible for the extreme locations of the MCC grades in the score plot (a). MCC property abbreviations are listed in Table 2.

3.7. Chemometric data analysis

All PCA and OPLS models were constructed with Simca-P+ version 12.0.1.0 (Umetrics, Umeå, Sweden). Some minor design interpretations (replicate plots) were performed with Modde version 9.0.0.0 (Umetrics).

4. Results and discussion

4.1. Selection of the MCC grades

Principal component analysis (PCA) was applied to the autoscaled physical properties (Table 3) of thirteen different MCC grades in order to select three extreme, i.e. the most dissimilar, grades and one center point. A large dissimilarity between the selected grades increases the chance that the resulting roll compacted products differ significantly and in theory multivariate calibration models should enable to predict the ribbon, granule or tablet properties of all MCC grades located more centrally in the PCA score plot. The constructed model contained two principal components explaining 78.3% of the variation in the MCC properties. From the PC1–PC2 score plot (Fig. 3a) it could be deduced that Avicel PH 101 was a representative center point, while Avicel PH105, Avicel PH 200 and Ceolus KG 1000 were located at the extreme ends of the score plot. Their extreme location implied that for some properties they exhibited values differing a lot from the average value of all MCC grades and therefore these grades were included in the design. The PC1–PC2 loading plot (Fig. 3b) indicated the properties responsible for the extreme location of the selected MCC grades: the Ceolus KG 1000 grade exhibited the lowest bulk density as well as a stability index and compressibility higher than most other grades, while Avicel PH 200 differed in basic flow energy, particle size distribution and bulk density. The flow rate index, permeability and specific energy of Avicel PH105 caused its extreme location in the score plot. The loading plot revealed that the variation of some variables, as for instance, particle sizes at 10 and 50% of the particle distribution and basic flowability energy, was correlated for these MCC grades.

4.2. Design interpretation with OPLS

In order to enhance information extraction from the experimental design, the qualitative factor, MCC grade, was transformed to several quantitative powder characteristics. These properties and the speed ratio, constituting the **X** matrix for modeling, were scaled to unit variance. A separate OPLS model was built for each property (**y**) of each roll compacted product (ribbons, granules, and tablets) describing the property **y** as a function of the design variation (**X**). The results are summarized in Table 4. No models were built to describe the powder blend properties, because it was assumed that they are totally correlated with the MCC properties. An important observation, however, was that the blends containing Ceolus KG 1000 or Avicel PH105 clearly exhibited a worse flowability. Fortunately, this did not cause problems for the roll compaction.

For some responses, e.g. ribbon density, very high R^2Y and Q^2 values were obtained (white columns in Table 4). This implied that these properties could be predicted very well from the variations introduced by the design. The fines percentage produced during roll compaction and the mass variation and the content uniformity of the tablets, however, exhibited very bad fits (low R^2Y and Q^2), which means that the main structured variation in these properties were introduced by other factors than MCC grade and speed ratio (dark columns in Table 4). The corresponding replicate plots for the tablets (Fig. 4) revealed that for these properties the variation between the center points was similar or even larger than the variation between the different batches, which confirms that the design factors did not have a significant effect on the response. Some properties, as for instance the particle size distribution of the granules, exhibited somewhat lower R^2Y and Q^2 values (light grey columns in Table 4). However, their model fit was still acceptable for interpretation.

For the first ribbon response, thickness, a good model could be fitted. The predictive component of the OPLS model explained 10% of the variation in the design (R^2X), while the structured variation contained in the two orthogonal components explained 81%. This means that a large part of the design variation did not influence the ribbon thickness. From the loading plot (Fig. 5) it could be deduced that only the speed ratio affected the ribbon thickness significantly. The thickness of the ribbons will thus increase by increasing the speed ratio during roll compaction, but changing the MCC grade has no effect. This was confirmed by the fact that four MCC properties were significant on the orthogonal components. From the significant factors in Table 4 and Fig. 5, it can be deduced that a higher flow rate index and a higher stability index of the MCC caused an increase in orthogonal variation. It was observed that Av 105 and Ceo 1000 exhibited extreme values for those properties, which caused their outlying behavior in the PC1–PC2 score plot (Fig. 3a). Although those grades exhibited a much higher flow rate index or stability index than the other grades and thus were responsible for a large part of the variation in the MCC properties, they will not result in ribbons with significantly different ribbon thickness. A low basic flowability energy and bulk density will also increase

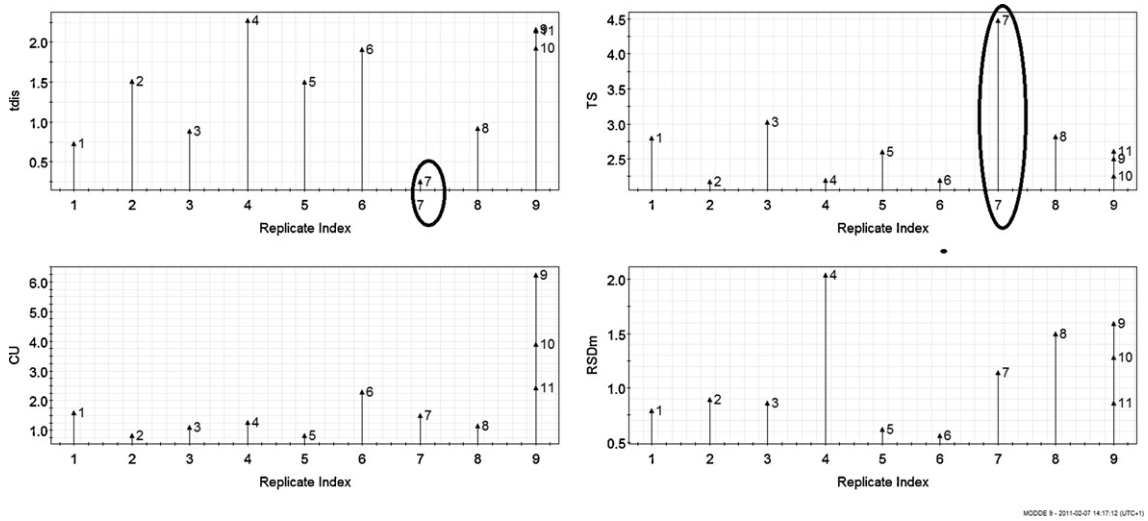

Fig. 4. Response plots for all measured tablet properties with the batch number (Table 1) indicated next to each arrow. The tablets from batch 7 (containing Ceolus KG-1000 and compacted at low speed ratio) exhibited more favorable tablet properties, i.e. a high tensile strength and a low disintegration time. The content uniformity and mass variation was similar for all batches. The response abbreviations are listed in Table 2.

orthogonal variation. The structured variation introduced in the design by changing the MCC grade not related with the response was thus separated from the predictive variation by using OPLS. For the ribbon density, very similar interpretations could be made. For ribbon porosity, Zinchuk et al. (2004) defined an optimal range from approximately 20 to 40% in order to produce granules with optimal compression properties leading to acceptable tablet quality. Within the studied design five batches fulfill this criterion (Table 5): two center points (located at upper border of optimal region), both Ceolus KG 1000 containing batches and the batch containing Avicel PH 101 compacted at high speed ratio. Except from the Ceolus KG 1000 based batch, all batches compacted at low speed ratio result in more porous ribbons. Higher porosities were also obtained for all batches containing Avicel PH105 and Avicel PH 200. The OPLS model predicting ribbon porosity exhibited a good fit and indicated that the speed ratio and the stability index and the bulk density of the MCC have a significant influence on the porosity.

The bulk density, flowability, compressibility and permeability of the granules could be predicted quite well by the OPLS models and were mainly influenced by the variation in the MCC properties. However, for the bulk density and permeability the speed ratio was also significant. From the signs of the loadings (positive versus neg-

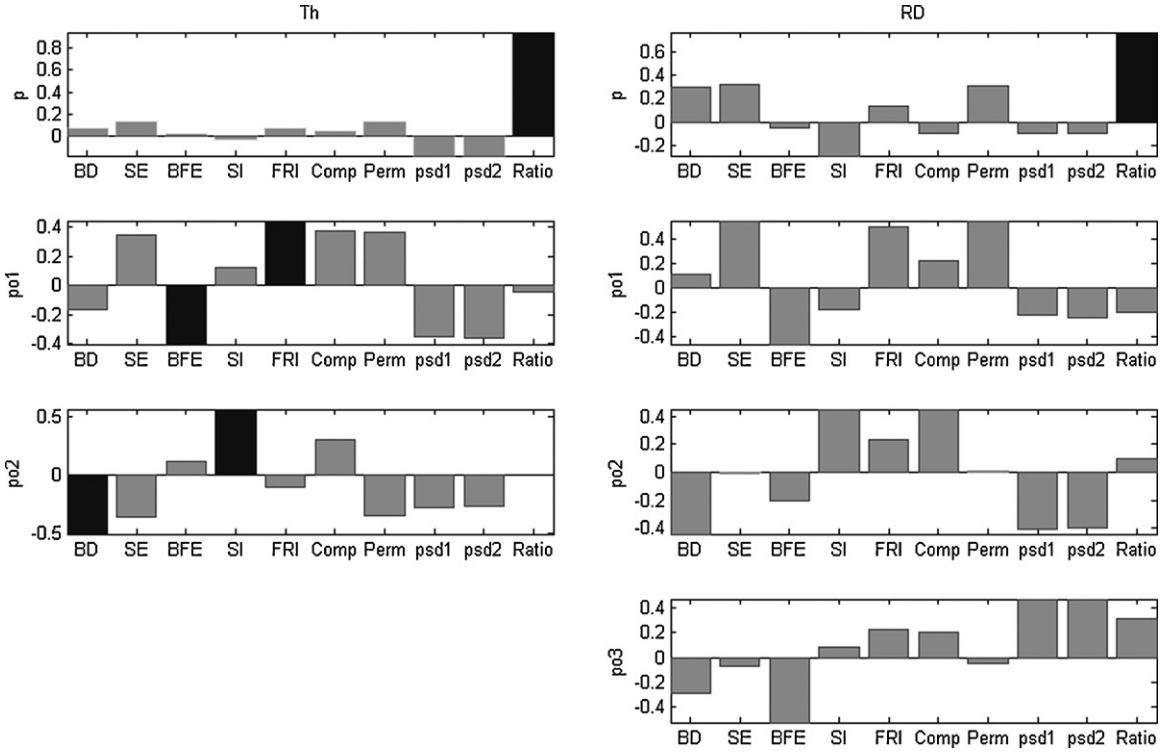

Fig. 5. Loading plots of the predictive (p) and orthogonal components (p_o) of the OPLS models predicting ribbon thickness and ribbon density from design variation with the significant loadings marked in black and all others in grey. The factor and response abbreviations are listed in Tables 1 and 2.

ative) we can deduce the direction of the factor effect. The loading interpretation was not straightforward for all responses. For the compressibility of the granules most MCC properties were significant on both predictive and orthogonal components. This indicates that the structured variation in those MCC properties is only partly related with the granule property. From the score plot (Fig. 6) it could be seen that batches 3 and 4 were responsible for the orthogonal variation, while batches 5–8 were responsible for the variation related with the compressibility of the resulting granules. Batches 3 and 4 (containing Av PH105) thus exhibited MCC properties deviating from the other MCC grades, but will not result in granules with significantly different compressibility. The presence of orthogonal components revealed again that a part of the structured variation in the design was not related with the granule properties.

The models for the particle size distribution of the granules exhibited a little worse fit, but it could still be deduced that the choice of MCC grade was influencing the particle size, while the speed ratio was not.

Considering the tablet properties, a good model could only be fit for the tensile strength. The loadings indicated that both the speed ratio and the MCC grade were significant factors on the predictive component, but the orthogonal loadings indicated that the variation in some of the MCC properties was not related to the tensile strength.

This study confirmed that OPLS separated the orthogonal variation from the predictive variation, which ensured that the predictive loadings were not confounded with uncorrelated systematic variation. This enabled an unambiguous interpretation of the factor effects, which could not be achieved by the interpretation of regression coefficients of PLS models. This statement could be illustrated with the tensile strength model, for which the regression coefficients of the PLS model indicated three significant factors: ratio, psd1 and psd2, while in the corresponding OPLS model psd1 and psd2 only exhibited significant loadings on the orthogonal component.

Our findings based on the OPLS models partially confirmed the results of the study of Herting and Kleinebudde (2007): raw materials with a smaller particle size will result in larger granules. This could be deduced from the loading plot of the OPLS model describing the median particle diameter (psd2) of the granules (Table 4). The 10th percentile of the particle size distribution curve (psd1) was not considered, because this measure is more related to the amount of fines. Contradictory to expectations and earlier findings, the OPLS model predicted a slower mass flow for granules produced from MCC grades with smaller particle size. This is probably caused by the Ceolus KG 1000 grade for which the lowest mass flow was obtained after roll compaction, although the granule particle size was high compared to the other batches (Table 5). Probably the large amount of air still present between the granules decreased the flowability. Since the particle size distribution of MCC was only significant on the orthogonal component of the OPLS model, it was not affecting the tablet tensile strength. This unexpected observation, contradicting the results of Herting and Kleinebudde (2007), could be caused by the inclusion of MCC grades with a larger particle size range in our study, which would imply that the relation between MCC particle size and tablet tensile strength is only valid in a small particle size range. Herting and Kleinebudde did not characterize other MCC properties, which make it difficult to explain our different results.

One other interesting type of information that can be retrieved from Table 4 was that the variation in the studied ribbon properties would not be sufficient to explain the tablet variation, because the ribbon properties were only influenced by the ratio, while tablet properties were influenced by both ratio and MCC grade. In order to avoid an extensive summation of all separate factor effects on each considered response, we refer to Table 4 for more detailed information.

4.3. Tablet quality throughout the design

The replicate plots (Fig. 4) indicated that the batch containing Ceolus KG 1000 roll compacted at a low speed ratio exhibited the lowest disintegration time and the highest tensile strength, which are two favorable tablet properties. Since all roll compacted batches disintegrated within 3 min (Table 5), the choice of MCC was not critical for the disintegration of this formulation. However, for another active the faster disintegration of Ceolus KG 1000 can make the difference between an acceptable and not acceptable tablet quality. RC 1, 3, 7, 8, 11 and all directly compressed batches resulted in tablets with acceptable tensile strength, when applying a lower limit of 2 MPa at a compaction pressure of less than 250 MPa (TSn = 8). The variation in mass between the different batches was similar to the variation between the center points, which implied that the mass variation was not significantly influenced by the design factors. This confirms the findings in Section 4.2. A similar observation could be made for content uniformity. From all studied MCC grades Ceolus KG 1000 could thus be considered most suited for roll compaction. This MCC grade exhibited the lowest bulk density and highest com-

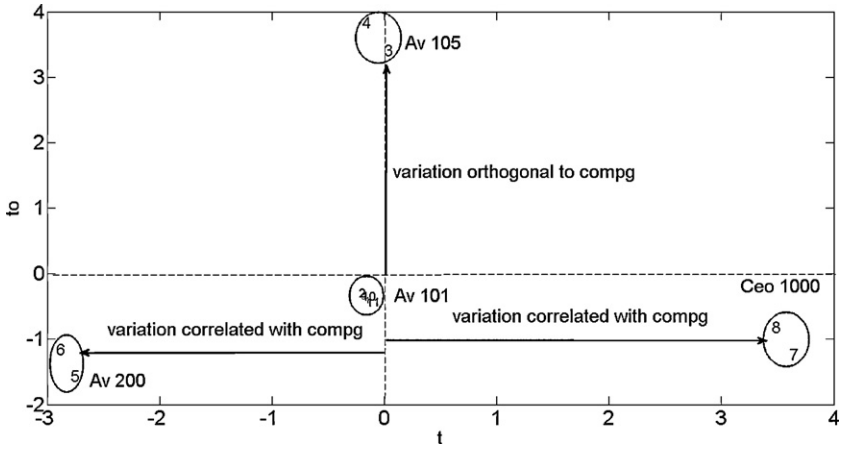

Fig. 6. Scores on the predictive component (t) versus the scores on the orthogonal component (t_o) of the OPLS model predicting the granule compressibility from design variation. The granule compressibility was varying along the predictive component of the OPLS model. The batches containing Avicel PH105 clearly exhibited variation not related with the compressibility of the resulting granules, while the batches containing Avicel PH200 and Ceolus KG1000 exhibited variation resulting in granules with different compressibility. Abbreviations are listed in Tables 1–3.

Table 4
Characteristics of the OPLS models constructed for each property of each roll compacted product, where pred stands for predictive component, orth for orthogonal component and *N* for the number of predictive/orthogonal components. The nature of the relationship between the significant factors and the response is indicated with a + or − sign between the brackets, while the number next to the significant orthogonal factors indicates the specific orthogonal component. The significant factors are ordered according to their loading magnitude. White columns indicate models with a good fit; the light grey columns indicate an acceptable fit and the dark grey a very bad fit. The response and factor abbreviations are listed in Tables 1 and 2.

Product	Ribbons				Granules						TABLETS			
response	Th	RD	Fin	*P*	BDg	Fg	Compg	Permg	Psd1g	Psd2g	t_{dis}	RSDm	TS	CU
R^2Y	0.971	0.958	0.662	0.952	0.957	0.973	0.839	0.922	0.731	0.706	0.700	0.457	0.879	0.147
Q^2	0.931	0.931	0.361	0.843	0.904	0.909	0.663	0.675	0.496	0.517	0.450	0.0724	0.576	0.0245
R^2X pred	0.10	0.13	0.50	0.229	0.19	0.34	0.42	0.29	0.51	0.49	0.21	0.509	0.22	0.43
N	1	1	1	1	1	1	1	1	1	1	1	1	1	1
R^2X orth	0.81	0.86	NA	0.771	0.72	0.57	0.39	0.64	NA	NA	0.70	NA	0.68	NA
N	2	3	0	3	2	2	1	2	0	0	2	0	2	0
Significant factors Pred	Ratio (+)	Ratio (+)	Comp (−) Psd1 (+) Psd2 (+) BD (+) SI (−) FRI (−) BFE (+)	SI (−) BD (+) Ratio (−)	BD (+) SI (−) Ratio (+)	BD (+) SI (−) Comp (−) Psd1 (+) Psd2 (+) BFE (+) FRI (−)	Comp (+) BD (−) SI (+) FRI (+) BFE (−) Psd1 (−) Psd2 (−)	Perm(+) SE (+) Ratio (+) FRI (+)	Psd1 (+) Psd2 (+) Comp (−) FRI (−) BFE (+)	FRI (+) Perm (+) SE (+) BFE (−) Comp (+) Psd2(−)	BD (+) Ratio (+) Comp (−) SI (−)	FRI (+) Comp (+) psd1 (−) psd2 (−) BFE (−)	BD (−) Ratio (−) Comp (+) SI (+) BFE (−)	BFE (+) FRI (−) Perm (−) SE (−) Psd2 (+)
Significant factors Orth	BFE (−,1) FRI (+,1) BD (−,2) SI (+,2)	–	NA	Comp (−,1) BFE (+,1) Psd1 (−,3) Psd2 (−,3)	–	SE (−,1) Perm (−,1) FRI (−,1) BFE (+,1) Psd2 (+,1) Comp (−,1) Ratio (−,2) SI (−,2) BD (+,2)	Perm (+,1) SE (+,1) FRI (+,1) BFE (−,1) SI (−,1) BD (+,1) Comp (+,1)	Comp (+,1) Psd1 (−,1) Psd2 (−,1) SE (+,2) Perm (+,2) SI (−,2)	NA	NA	Psd1 (+,1) Psd2 (+,1) FRI (−,1) Comp (−,1) Perm (+,2) SE (+,2) SI (−,2) FRI (+,2) BD (+,2)	NA	FRI (+,1) Psd2 (−,1) Psd1 (−,1) Comp (+,1) BFE (−,1)	NA

Table 5
Tablet properties of the directly compressed (DC) batches and characteristics of the roll compacted products (powder blends, ribbons, granules and tablets) obtained within the full factorial design. The batch and property abbreviations are listed in Tables 1 and 2, while the MCC grade abbreviations are listed in Table 3.

Batch	Powder blends						Ribbons				Granules						Tablets				
	BD	*F*	Comp	Perm	psd1	psd2	Th	RD	Fin	*P*	BDg	Fg	Compg	Permg	psd1g	psd2g	t_{dis}	RSDm	TS	TSn	CU
RC 1	0.50	9.31	23.7	1.3	18.4	70.8	1.0	0.92	21	43.8	0.58	16.8	11.1	0.82	34.5	244.1	0.73	0.79	2.80	9.52	1.60
RC 2	0.50	9.31	23.7	1.3	18.4	70.8	1.2	1.15	20	30.1	0.68	20.7	14.5	1.57	31.3	431.7	1.51	0.89	2.17	5.37	0.83
RC 3	0.52	0.85	27.2	7.8	6.7	28.7	1.0	0.99	18	53.0	0.62	16.3	13.6	1.23	26.6	672.6	0.88	0.86	3.03	10.84	1.09
RC 4	0.52	0.85	27.2	7.8	6.7	28.7	1.2	1.17	21	44.9	0.70	22.8	14.0	2.43	24.1	662.3	2.28	2.04	2.19	5.39	1.26
RC 5	0.52	16.40	14.0	0.4	58.5	202.6	1.0	0.88	43	53.5	0.56	23.2	7.4	0.35	56.8	217.2	1.50	0.62	2.60	7.94	0.81
RC 6	0.52	16.40	14.0	0.4	58.5	202.6	1.2	1.09	26	42.0	0.64	25.6	9.0	0.64	39.1	226.3	1.91	0.56	2.19	6.07	2.28
RC 7	0.27	0.81	29.6	0.8	12.7	49.7	1.0	0.80	17	39.1	0.38	9.2	25.0	0.47	23.4	171.1	0.25	1.14	4.48	17.94	1.50
RC 8	0.27	0.81	29.6	0.8	12.7	49.7	1.2	1.04	15	20.7	0.53	14.5	18.6	1.16	30.4	579.9	0.92	1.50	2.82	9.18	1.15
RC 9	0.50	9.31	23.7	1.3	18.4	70.8	1.1	1.00	19	39.0	0.64	19.3	13.8	1.12	33.2	293.2	2.16	1.59	2.50	6.49	6.24
RC 10	0.50	9.31	23.7	1.3	18.4	70.8	1.2	1.04	22	36.8	0.65	18.9	10.7	1.23	30.0	255.7	1.93	1.28	2.25	5.57	3.90
RC 11	0.50	9.31	23.7	1.3	18.4	70.8	1.1	0.97	18	41.1	0.60	19.9	12.6	0.96	31.7	213.2	2.14	0.86	2.61	9.15	2.43
DC Av PH101	0.50	9.31	23.7	1.3	18.4	70.8											0.54	1.52	3.40	16.92	7.21
DC Av PH105	0.52	0.85	27.2	7.8	6.7	28.7											0.73	4.18	4.16	18.09	3.89
DC Av PH200	0.52	16.40	14.0	0.4	58.5	202.6											1.24	0.84	2.73	8.69	8.57
DC Ceo 1000	0.27	0.81	29.6	0.8	12.7	49.7											–	–	–	–	–

pressibility from the thirteen characterized grades (Table 3), which might cause its favorable behavior during roll compaction. Also its stability index was rather high compared to most other MCC grades. However, the Ceolus KG 1000 resulted in powder blends, which were somewhat more difficult to handle due to the fluffiness (indicated by the low bulk density in Table 5) and the bad flowing properties (indicated by the low mass flow value in Table 5).

The replicate plots reveal some general tendencies also indicated by the OPLS models: an increase in applied speed ratio will result in tablets with higher tensile strength, but also with a longer disintegration time. Batches containing Avicel PH105 and Avicel PH 200 resulted in tablets with higher disintegration times. The different MCC grades resulted in tablets with quite similar tensile strengths, except Ceolus KG 1000. It can be thus concluded that the design variation resulted in quality differences between the batches and only RC 1, 3, 7, 8 and 11 resulted in acceptable drug formulations.

4.4. Roll compaction versus direct compression

Unfortunately, the batches containing Ceolus KG 1000 could not be directly compressed probably due to the large amount of air between the particles and the low bulk density of the blend. Since the resulting tablets fell apart immediately after tabletting, even when the highest applicable press force was used, the batch had to be excluded from this comparison. The disintegration time and weight variation of all other directly compressed (DC) tablet batches fell within the range of the values obtained for roll compacted tablets. For these two properties there was thus no significant difference between the two different tablet manufacturing procedures. However, the average of the content uniformity values of all three directly compressed batches (6.6%) was obviously higher than for average of the 11 roll compacted batches (2.1%), which points out the worse content uniformity. The tensile strength (Table 5), on the contrary, was as expected better, i.e. higher, for the directly compressed tablets compared to the roll compacted batches. However, the batch containing Ceolus KG-1000 compacted at low speed ratio exhibited the highest normalized tensile strength, i.e. the average tensile strength of ten tablets with an aimed crushing strength of 80 N normalized with the applied compaction pressure.

An OPLS model was constructed to describe the reduction in tablet tensile strength after roll compaction as a function of the applied speed ratio and the difference in physical properties of granules and powder blends. This reduction was expressed as the tensile strength ratio (TS ratio), i.e. TS roll compacted batch/TS directly compressed batch. A low TS ratio indicates thus a large decrease in tensile strength. The batches containing Ceolus KG-1000 were excluded, because, as mentioned earlier, they could not be compressed directly. The obtained model contains one predictive component ($R^2X = 0.455$) and two orthogonal components ($R^2X = 0.369$ and 0.141) and exhibits a good fit ($R^2Y = 0.965$, $Q^2 = 0.989$). From the predictive loading plot it could be deduced that a larger increase in mass flow, bulk density and particle size (psd1 and 2) after granulation will result in a larger tensile strength reduction (lower TS ratio). This confirms the results of Herting and Kleinebudde (2008) and Sun and Himmelspach (2006). Additionally, the loading plot indicated that the compressibility decrease after roll compaction, represented by the difference between powder blend and granule compressibility, correlates with the tensile strength reduction. Those significant factors are all correlated with the change in median particle size (psd2) after granulation: flowability ($R^2 = 0.77$), compressibility ($R^2 = 0.43$), bulk density ($R^2 = 0.58$) and particle size at 10% of the distribution ($R^2 = 0.44$). The increase in particle size after roll compaction will thus be largely responsible for the reduction in tensile strength. However, the lower correlation values for compressibility and bulk density support the findings of Herting and Kleinebudde (2008), which states that also work hardening is involved.

5. Conclusions

The introduction of MCC properties as quantitative factors in the design of experiments instead of including the MCC grade as a qualitative factor resulted in many new insights of the influence of raw material properties on the roll compaction process. The use of OPLS models to link the MCC properties to the properties of the roll compacted products facilitated the design interpretation compared to PLS. The speed ratio had a significant effect on all ribbon and tablet properties, but only on some granule properties. The MCC grade on the other hand was significant for all granule and tablet properties, but only for one ribbon property, which was porosity. The bulk density and the compressibility were the most influencing properties of the MCC. Our study confirmed that MCC with smaller particle size results in larger granules after roll compaction, but contradicted that this increase in size always results in a better flowability as observed by Herting and Kleinebudde (2007). The constructed OPLS models also make it possible to estimate the roll compaction properties of newly introduced MCC grades.

The roll compacted tablets exhibited better content uniformity than the directly compressed tablets. All tablets, except the ones containing Ceolus KG-1000, exhibited lower tensile strengths after roll compaction due to the double compaction. The OPLS model describing the tensile strength reduction indicates that the increase in particle size is largely responsible for this reduced compactibility. However, there are also indications that other mechanisms are involved, as stated by Herting and Kleinebudde.

Finally, the evaluation of the full factorial design pointed out clearly that the Ceolus KG-1000 resulted in better tablets, i.e. higher tensile strength and shorter disintegration time, compared to the other MCC grades. However, this raw material was more difficult to handle due to its fluffiness.

Acknowledgements

AstraZeneca is acknowledged for the financial support as well as for placing their laboratories and formulation experts at our disposal.

References

Am Ende, M.T., Moses, S.K., Carella, A.J., Gadkari, R.A., Graul, T.W., Otano, A.L., Timpano, R.J., 2008. Improving the content uniformity of a low-dose tablet formulation through roller compaction optimization. Pharm. Dev. Technol. 12, 391–404.

Bacher, C., Olsen, P.M., Bertelsen, P., Kristensen, J., Sonnergaard, J.M., 2007. Improving the compaction properties of roller compacted calcium carbonate. Int. J. Pharm. 342, 115–123.

Bindhumadhavan, G., Seville, J.P.K., Adams, M.J., Greenwood, R.W., Fitzpatrick, S., 2005. Roll compaction of a pharmaceutical excipient: experimental validation of rolling theory for granular solids. Chem. Eng. Sci. 60, 3891–3897.

Bultmann, J.M., 2002. Multiple compaction of microcrystalline cellulose in a roller compactor. Eur. J. Pharm. Biopharm. 54, 59–64.

Dec, R.T., Zavaliangos, A., Cunningham, J.C., 2003. Comparison of various modeling methods for analysis of powder in roller press. Powder Technol. 130, 265–271.

Falzone, A.M., Peck, G.E., McCabe, G.P., 1992. Effects of changes in roller compactor parameters on granulations produced by compaction. Drug Dev. Ind. Pharm. 18, 469–489.

Farber, L., Hapgood, K.P., Michaels, J.N., Fu, X., Meyer, R., Johnson, M., Li, F., 2008. Unified compaction curve model for tensile strength of tablets made by roller compaction and direct compression. Int. J. Pharm. 346, 17–24.

Freeman, R., 2007. Measuring the flow properties of consolidated, conditioned and aerated powders – a comparative study using a powder rheometer and a rotational shear cell. Powder Technol. 174, 25–33.

Herting, M.G., Kleinebudde, P., 2007. Roll compaction/dry granulation: effect of raw material particle size on granule and tablet properties. Int. J. Pharm. 338, 110–118.

Herting, M.G., Kleinebudde, P., 2008. Studies on the reduction of tensile strength of tablets after roll compaction/dry granulation. Eur. J. Pharm. Biopharm. 70, 372–379.
Hervieu, P., Dehont, F., Jerome, E., Delacoure, A., Guyot, J.C., 1994. Granulation of pharmaceutical powders by compaction an experimental study. Drug Dev. Ind. Pharm. 20, 65–74.
Jeon, I., Maurya, B., Gilli, T., Vandamme, T.F., Bertz, G., 2009. How to minimize the limitations of roll compaction. Pharm. Technol. 21, 31–34.
Johanson, J.R., 1965. A rolling theory for granular solids. J. Appl. Mech. 32, 842–848.
Kleinebudde, P., 2004. Roll compaction/dry granulation: pharmaceutical applications. Eur. J. Pharm. Biopharm. 58, 317–326.
Malkowska, S., Khan, K.A., 1983. Effect of recompression on the properties of tablets prepared by dry granulation. Drug Dev. Ind. Pharm. 9, 331–347.
Massart, D.L., Vandeginste, B.G.M., Buydens, L.M.C., De Jong, S., Lewi, P.J., Smeyers-Verbeke, J., 1998. Relations between measurement tables. In: Handbook of Chemometrics and Qualimetrics, Part B. Elsevier, Amsterdam, pp. 307–348(Chapter 35).
Reynolds, G., Ingale, R., Roberts, R., Kothari, S., Gururajan, B., 2010. Practical application of roller compaction process modeling. Comput. Chem. Eng. 34, 1049–1057.
Sun, C.C., Himmelspach, M.W., 2006. Reduced tabletability of roller compacted granules as a result of granule size enlargement. J. Pharm. Sci. 95, 200–206.
Teng, Y., Qiu, Z., Wen, H., 2009. Systematical approach of formulation and process development using roller compaction. Eur. J. Pharm. Biopharm. 73, 219–229.
Trygg, J., Wold, S., 2002. Orthogonal projections to latent structures (O-PLS). J. Chemometr. 16, 119–128.
Zinchuk, A.V., Mullarney, M.P., Hancock, B.C., 2004. Simulation of roller compaction using a laboratory scale compaction simulator. Int. J. Pharm. 269, 403–415.